THE JOURNAL OF PHYSICAL CHEMISTRY B

Article

pubs.acs.org/JPCB

Ionic-Liquid-Induced Changes in the Properties of Aqueous Zwitterionic Surfactant Solution: Solvent and Rotational Relaxation Studies

Vishal Govind Rao, Chiranjib Ghatak, Surajit Ghosh, Sarthak Mandal, and Nilmoni Sarkar*

Department of Chemistry, Indian Institute of Technology, Kharagpur 721302, West Bengal, India

ABSTRACT: In the recent past, the chameleon-like nature of zwitterionic micelles has been utilized for performing electrophilic, nucleophilic, base, and acid catalyzed reactions. But the use of simple salts to induce the zwitterionic character limits the variation to inorganic cations and anions only. To overcome this problem, we have used room temperature ionic liquids (RTILs), which can be tailored according to need. More precisely, we have shown the effect of added RTILs on the nature of water molecules in the palisade layer of a zwitterionic (*N*-hexadecyl-*N*,*N*-dimethylammonio-1-propanesulfonate (SB-16)) micelle using solvation and rotational relaxation studies of C-153 dye. We have carried out a comparative study of changes in the solvent and rotational relaxation parameters of C-153 in an aqueous solution of SB-16 upon addition of three different ionic liquids (ILs): 1-ethyl-3-methylimidazolium ethyl sulfate $[C_2mim][C_2SO_4]$, 1-ethyl-3-methylimidazolium *n*-butyl sulfate $[C_2mim][C_4SO_4]$, and 1-ethyl-3-methylimidazolium *n*-hexyl sulfate $[C_2mim][C_6SO_4]$. It has been observed that in the presence of added RTILs the solvation dynamics become faster and the change in solvation dynamics is more pronounced in the case of $[C_2mim][C_6SO_4]$ compared to that for $[C_2mim][C_4SO_4]$ and $[C_2mim][C_2SO_4]$. This can be accounted for by considering the increased water penetration (increased microfluidity) with the addition of ILs. In accordance with solvation dynamics results, fluorescence anisotropy studies also indicate an increase in microfluidity of the palisade layer of the SB-16 micelle with the added RTILs. The average rotational relaxation time in 28 mM SB-16 was found to be 1.12 ns. With the addition of 800 mM $[C_2mim][C_2SO_4]$, the average rotational relaxation time remains the same (1.12 ns), whereas with the addition of 800 mM $[C_2mim][C_6SO_4]$ it decreases to 0.40 ns. This observation is in agreement with our earlier report on the microfluidity of SB-16 solution with the addition of $[C_2mim][C_2SO_4]$ and $[C_2mim][C_6SO_4]$ (Rao, V. G.; Ghatak, C.; Ghosh, S.; Mandal, S.; Sarkar, N. *Chem. Phys. Chem.* DOI: 10.1002/cphc.201100866).

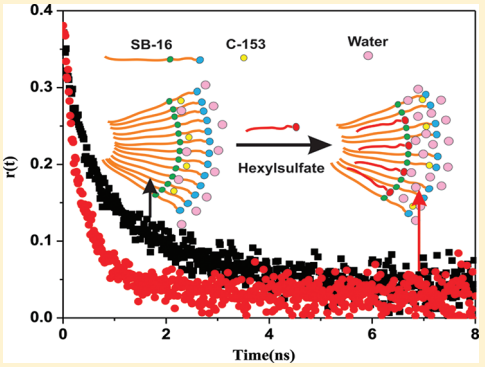

1. INTRODUCTION

Information regarding the time-dependent behavior of solvent molecules (solvation dynamics) in response to a changing charge distribution such as a newly created ion, dipole, or multipole within different micellar solutions is quite important for a better insight into chemical reactions such as electron-transfer and charge-transfer processes in these organized environments. The nature exhibited by water molecules present at the interface of microscopic confined environments such as interface of micelles, proteins, DNA, etc., is distinctly different from bulk water behavior. The divergent properties vary from exhibiting interesting and diverse structures to dynamics that are different from what is observed in the bulk. In recent times, there has been much interest in biological water molecules in the hydration layer that surrounds self-assemblies and proteins in aqueous solutions.[1−7] What makes it so attention grabbing is that the stability and function of these self-assemblies and biomolecules depend on the structure and dynamics of such biological water. Hence, it is essential to understand the time scales for water dynamics and how these aqueous solutions crucially depend on them.

Needless to say, considerable efforts have been made in this direction for many years.[4−6,8−20] Owing to the extensive studies on solvation dynamics in different heterogeneous media such as micelles, reverse micelles, lipids, proteins, DNA, etc.,[4−6,13−20] the solvation dynamics study of a newly created ion or a dipole in polar liquids is now a well-established method for obtaining molecular level information about the response of solvent molecules (which comprises both orientational and translational motions) to the probe.[4−6,21−24] The time scale of response of solvent molecules to rearrange around solute molecules has a critical influence on the rates of chemical reactions in liquids.[25] The uniqueness of solvation dynamics as a probe is that it allows, at least partly, for discrimination between the local and global contributions.

So far, both experimental[16,26−30] and computational[31−39] methods have been used to exploit solvation dynamics in micelles of different surfactants. Popular probes for experimental studies include coumarin 480 (C-480), coumarin 153

Received: January 17, 2012
Revised: February 27, 2012
Published: March 1, 2012

Scheme 1. Structures of ILs: $[C_2mim][C_2SO_4]$, $[C_2mim][C_4SO_4]$, and $[C_2mim][C_6SO_4]$, Fluorescence Probe Coumarin 153, and Zwitterionic Surfactant SB-16

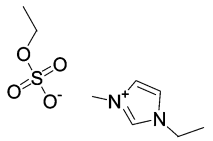

1-Ethyl-3-methylimidazolium ethylsulfate
$[C_2mim][C_2SO_4]$

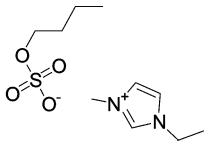

1-Ethyl-3-methylimidazolium n-butylsulfate
$[C_2mim][C_4SO_4]$

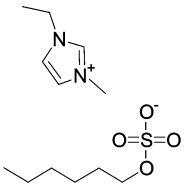

1-Ethyl-3-methylimidazolium n-hexylsulfate
$[C_2mim][C_6SO_4]$

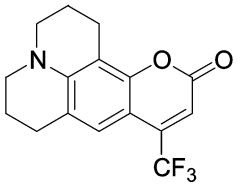

Coumarin 153 (C-153)

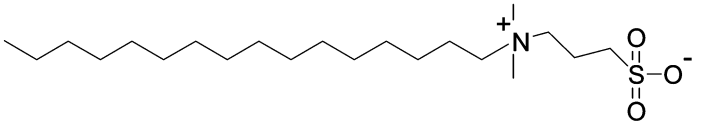

SB-16

(C-153), coumarin 343 (C-343), and 4-aminophthalimide (4-AP) since the emission properties of these probes in micelles are very different from those in bulk water. The studies[26−39] clearly show that the solvation dynamics in the Stern layer of a micelle could be 2 orders of magnitude slower than that in bulk water. Investigation of the dynamics of water molecules in the hydration layer also reveals the coexistence of both fast (of the order of a few picoseconds) and slow (estimates vary from tens of picoseconds to nanoseconds) components. According to the famous phenomenological model of Nandi and Bagchi, the origin of this bimodal dynamics can be (partly) rationalized in terms of "bound" (by hydrogen bonding, to macromolecular surface) and "free" water molecules in the layer.[21] The amplitudes and time scales of motion in the hydration layer are determined by interconversion (that is, the HB breaking) kinetics among these species. Not only this, the water molecules at the interface can be molded by the shape fluctuations of micelles and the side-chain motions of proteins.[40−44] The knowledge of charge distribution on the macromolecular surface is essential to determining the relationship between the macromolecule and water molecule. Depending on the extent and nature of charge distribution the orientation and strength of the water molecule changes which is reflected in both the dynamics and phase behavior of surfactant solutions.[45−52]

In recent years, zwitterionic micellar systems have emerged as another common and widely studied example of restricted environment.[53−67] The zwitterionic surfactants, such as sulfobetaines and carboxybetaines, are formally neutral, but their micelles incorporate anions owing to the higher charge density of the cationic ammonium inner surface, compared with that of the anionic sulfonate or carboxylate surface.[53−61] Due to these unique properties they are quite useful in separation processes. By using packed zwitterionic columns for liquid chromatography, one can separate inorganic anions or cations,[68,69] and acidic or basic proteins,[70] both independently and simultaneously in a single run using optimum conditions. Furthermore, the chameleon-like nature of zwitterionic micelles can be utilized for performing electrophilic, nucleophilic, base, and acid catalyzed reactions.[71,72]

To further increase the utility of the zwitterionic micelles, we have investigated the effect of ionic liquid (IL) addition on their properties. The zwitterionic character may be introduced into the micelles using simple salts which would entail the use of inorganic cations and anions only. To obtain flexibility in the choice of cations and anions, one can make use of ionic liquids (ILs). This provides the added advantage of having control over the structure of these ions since ILs can be designed to our goal. In addition, modification of the physicochemical properties of aqueous surfactant solutions in favorable fashion by the addition of environmentally benign room-temperature ionic liquid (RTIL) has received enormous attention.[73−76] Due to its unusual properties, an IL may demonstrate a unique role in altering the properties of aqueous surfactant solutions. In our earlier paper,[77] we established the role of the alkyl chain length of the anion of the added ionic liquids on (i) the incorporation of anions in zwitterionic micelles (selectivity of anions) and (ii) the physicochemical properties of aqueous solution of SB-16. In this paper, we show the effect of added RTILs on the nature of water molecules in the palisade layer of a zwitterionic (*N*-hexadecyl-*N*,*N*-dimethylammonio-1-propanesulfonate (SB-16)) micelle using solvation and rotational relaxation studies of C-153 dye. Using three different ionic liquids (ILs), 1-ethyl-3-methylimidazolium ethyl sulfate $[C_2mim][C_2SO_4]$, 1-ethyl-3-methylimidazolium *n*-butyl sulfate $[C_2mim][C_4SO_4]$, and 1-ethyl-3-methylimidazolium *n*-hexyl sulfate $[C_2mim][C_6SO_4]$, we have carried out a comparative study of their effects on the solvent and rotational relaxation parameters of C-153 in an aqueous solution of SB-16.

dx.doi.org/10.1021/jp300544j | J. Phys. Chem. B 2012, 116, 3690−3698

2. EXPERIMENTAL SECTION

2.1. Materials and Sample Preparation. Coumarin 153 (C-153) (laser grade, Exciton) was used as received. SB-16 was purchased from Sigma-Aldrich and used as received. $[C_2mim][C_2SO_4]$, $[C_2mim][C_4SO_4]$, and $[C_2mim][C_6SO_4]$ were obtained from Bioniqs (>99% purity) and were also used as received. Doubly distilled deionized water (Milli-Q water) was used for sample preparation. The stock solution of C-153 was prepared in methanol. The final concentration of the probe molecule, C-153, in all the measurements was kept at $\sim 2.5 \times 10^{-6}$ M. Aqueous SB-16 solutions of the probe were prepared taking appropriate aliquots of the probe from the stock and evaporating methanol using a stream of nitrogen gas. Aqueous SB-16 of desired concentration was then added to achieve the required final probe concentration. Calculated amounts of ILs were added directly to the aqueous SB-16 solutions. All the experiments were performed at 298 K. The structures of $[C_2mim][C_2SO_4]$, $[C_2mim][C_4SO_4]$, and $[C_2mim][C_6SO_4]$, zwitterionic surfactant SB-16, and coumarin 153 are shown in Scheme 1.

2.2. Instrumentation. The absorption and fluorescence spectra were collected using a Shimadzu (model no. UV-2450) spectrophotometer and a Hitachi (model no. F-7000) spectrofluorimeter, respectively. For steady-state experiments, all the samples were excited at 410 nm. The detailed time-resolved fluorescence setup is described in our earlier publication.[78−80] Briefly, the samples were excited at 408 nm using a picosecond laser diode (IBH, Nanoled), and the signals were collected at the magic angle (54.7°) using a Hamamatsu microchannel plate photomultiplier tube (3809U). The instrument response function of our setup is ~90 ps. The same setup was used for anisotropy measurements. For the anisotropy decays, we used a motorized polarizer on the emission side. The emission intensities at parallel $I_{\parallel}(t)$ and perpendicular $I_{\perp}(t)$ polarizations were collected alternatively until a certain peak difference between parallel $I_{\parallel}(t)$ and perpendicular $I_{\perp}(t)$ decay was reached. The analysis of the data was done using IBH DAS, version 6 decay analysis software. The same software was also used to analyze the anisotropy data. The temperature was kept constant (298 K) by circulating water through the cell holder using a Neslab Thermostat (RTE7).

3. RESULTS AND DISCUSSION

3.1. Steady-State Studies. The absorption and emission spectra of C-153 in 28 mM aqueous SB-16 in the presence of different amounts of ILs were recorded at 298 K. A gradual red shift in the absorption maximum is observed with the addition of ILs in the micellar system. The absorption spectra of C-153 in 28 mM aqueous SB-16 in the presence of different amounts of $[C_2mim][C_6SO_4]$ are shown in the Figure 1. The emission maximum is blue-shifted from its value of 550 nm in neat water to 536 nm with the addition of 28 mM SB-16 in water. Thus, we can say the microenvironment experienced by C-153 in the micelle is different from neat water and the polarity experienced by C-153 is less than that in neat water. A gradual red shift is observed in emission spectra with the addition of ILs in the micellar system. The maximum red shift is observed in case of $[C_2mim][C_6SO_4]$ addition. The emission maximum is red-shifted from 536 to 541 nm with the addition of 800 mM $[C_2mim][C_6SO_4]$ to 28 mM aqueous SB-16 (Figure 2). The increased micellar hydration could be the one of the reasons responsible for the red shift with the addition of RTILs. It is

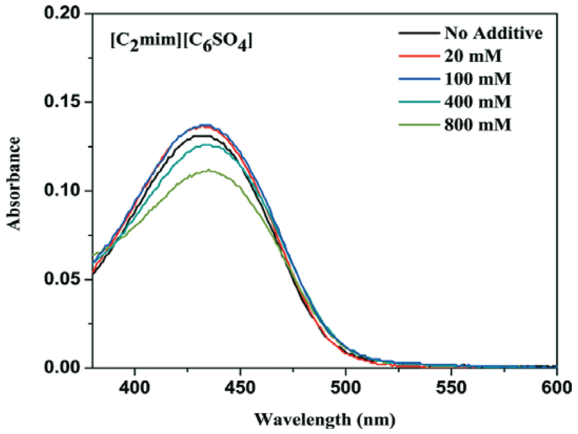

Figure 1. Absorption spectra of C-153 in 28 mM aqueous SB-16 in the presence of different amounts of $[C_2mim][C_6SO_4]$.

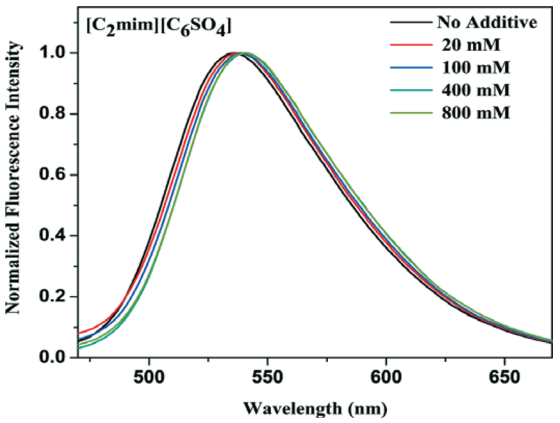

Figure 2. Emission spectra of C-153 in 28 mM aqueous SB-16 in the presence of different amounts of $[C_2mim][C_6SO_4]$.

inferred that, as micellar hydration increases, the probe in the palisade layer undergoes a relative migration toward the micellar surface, causing it to experience more polar microenvironment. From absorption and steady-state fluorescence spectra, it is also seen that the spectral width remains almost unaffected with the addition of RTILs, suggesting that the distribution of the dye molecules in the palisade layer is not altered significantly by the presence of the RTILs.

3.2. Time-Resolved Studies. *3.2.1. Time-Resolved Anisotropy Studies.* Absorption and emission spectra can give a qualitative idea regarding the location of the probe molecules. This can be more accurately predicted by the time-resolved fluorescence anisotropy. The fluorescence anisotropy decay of the organic dye molecules is directly related to the reorientation dynamics of excited molecule and hence it is the best suited technique for investigation of molecular dynamics near the site of dye molecule. Time-resolved fluorescence anisotropy $r(t)$ is calculated using the following equation

$$r(t) = \frac{I_{\parallel}(t) - GI_{\perp}(t)}{I_{\parallel}(t) + 2GI_{\perp}(t)} \quad (1)$$

where G is the correction factor for detector sensitivity to the polarization direction of emission and $I_{\parallel}(t)$ and $I_{\perp}(t)$ are fluorescence decays polarized parallel and perpendicular to the polarization of the excitation light, respectively. The fluorescence anisotropy decays of C-153 in 28 mM aqueous SB-16

dx.doi.org/10.1021/jp300544j | J. Phys. Chem. B 2012, 116, 3690−3698

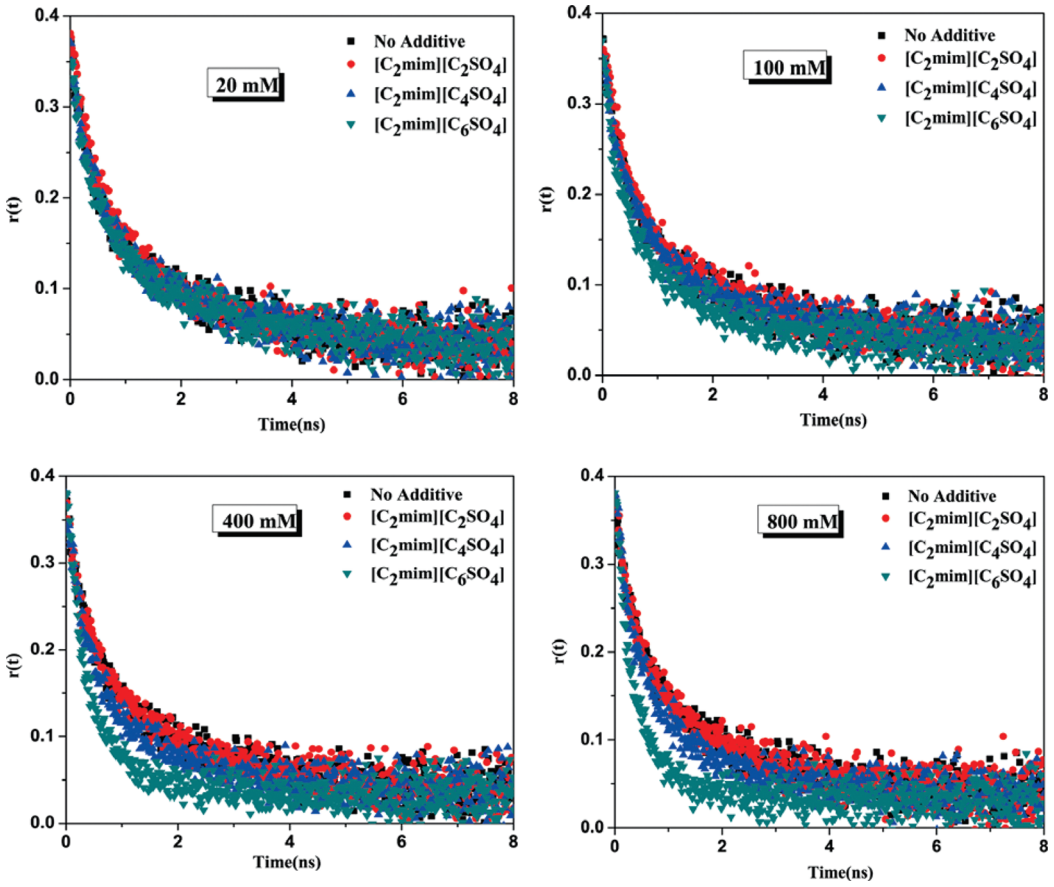

Figure 3. Time-resolved fluorescence anisotropy decay of C-153 in 28 mM aqueous SB-16 in the presence of different amounts of ILs.

Table 1. Anisotropy Decay Parameters of C-153 in 28 mM Aqueous SB-16 in the Presence of Different Amounts of ILs

additive concn (mM)	additive	a_{slow}	τ_{slow} (ns)	a_{fast}	τ_{fast} (ns)	$\langle\tau_{rot}\rangle$ (ns)[a]	r_0	viscosity (cP)[a]
0	no additive	0.48	1.95	0.52	0.35	1.12	0.37	0.92
20	$[C_2mim][C_2SO_4]$	0.50	1.78	0.50	0.32	1.05	0.38	0.95
	$[C_2mim][C_4SO_4]$	0.42	2.28	0.58	0.40	1.19	0.37	0.97
	$[C_2mim][C_6SO_4]$	0.43	2.13	0.57	0.36	1.12	0.35	1.02
100	$[C_2mim][C_2SO_4]$	0.45	2.30	0.55	0.38	1.24	0.36	1.00
	$[C_2mim][C_4SO_4]$	0.46	1.91	0.54	0.36	1.07	0.35	1.05
	$[C_2mim][C_6SO_4]$	0.51	1.24	0.49	0.20	0.73	0.37	1.07
400	$[C_2mim][C_2SO_4]$	0.47	2.03	0.53	0.34	1.13	0.37	1.04
	$[C_2mim][C_4SO_4]$	0.36	1.81	0.64	0.36	0.88	0.38	1.22
	$[C_2mim][C_6SO_4]$	0.35	0.88	0.65	0.23	0.46	0.38	1.40
800	$[C_2mim][C_2SO_4]$	0.44	2.07	0.56	0.37	1.12	0.37	1.36
	$[C_2mim][C_4SO_4]$	0.51	1.17	0.49	0.22	0.70	0.38	1.65
	$[C_2mim][C_6SO_4]$	0.46	0.65	0.54	0.19	0.40	0.38	2.18

[a]Error in experimental data of ±5%. Taken from our earlier publication.[77]

in the presence of different amounts of ILs, $[C_2mim][C_2SO_4]$, $[C_2mim][C_4SO_4]$, and $[C_2mim][C_6SO_4]$ are shown in Figure 3. All the fluorescence anisotropy decays of C-153 were fitted to a biexponential function. The biexponential nature of rotational relaxation arises due to different kinds of motion of the probe molecule in the micelle. This biexponential nature can be explained by the two-step model and the wobbling-in-a cone model. The two-step model proposes that the observed slow rotational relaxation (τ_{slow}) is a convolution of the relaxation time corresponding to the overall rotational motion of the micelles (τ_M) and lateral diffusion of the probe (τ_D). The wobbling-in-a-cone model describes the internal motion of the probe (τ_e) in terms of a cone angle (θ_0) and wobbling diffusion coefficient (D_w). These parameters are calculated from the relevant equations defined by Quitevis et al.[81]

$$\frac{1}{\tau_{slow}} = \frac{1}{\tau_D} + \frac{1}{\tau_M} \quad (2)$$

$$\frac{1}{\tau_{fast}} = \frac{1}{\tau_e} + \frac{1}{\tau_{slow}} \quad (3)$$

τ_{slow} and τ_{fast} are the observed fast and slow components of rotational relaxation. The anisotropy results are summarized in Table 1. For obtaining all the parameters discussed above, we

dx.doi.org/10.1021/jp300544j | J. Phys. Chem. B 2012, 116, 3690−3698

Table 2. Analytical Rotational Parameters Obtained from the Anisotropy Decays of C-153 in 28 mM Aqueous SB-16 in the Presence of Different Amounts of ILs

additive concn (mM)	additive	τ_m (ns)	τ_e (ns)	τ_D (ns)	$D_W \times 10^{-8}$ (s^{-1})	$D_L \times 10^6$ (cm^2 s^{-1})	θ_0 (deg)	S	η_{mic} (cP)
0	no additive	47.49	0.427	2.034	3.158	11.22	39.04	0.69	18.80
20	$[C_2mim][C_2SO_4]$	23.61	0.390	1.925	3.258	7.28	37.6	0.71	17.62
	$[C_2mim][C_4SO_4]$	13.66	0.485	2.737	3.205	3.51	41.84	0.65	19.98
	$[C_2mim][C_6SO_4]$	8.32	0.433	2.864	3.492	2.33	41.15	0.66	18.80
800	$[C_2mim][C_2SO_4]$	102.67	0.451	2.113	3.306	13.91	40.94	0.66	18.80
	$[C_2mim][C_4SO_4]$	115.88	0.271	1.182	4.547	23.70	37.31	0.71	11.75
	$[C_2mim][C_6SO_4]$	23.65	0.268	0.668	5.272	12.08	39.89	0.68	6.71

need to know the value of τ_M, which can be calculated from the Stokes−Einstein−Debye relation

$$\tau_M = \frac{\eta 4\pi {r_h}^3}{3kT} \quad (4)$$

where η is the viscosity of the bulk medium, r_h is hydrodynamic radius of the micelle, and k and T are the Boltzmann constant and absolute temperature, respectively. From Table 2, it is clear that the τ_M values are quite high compared to the τ_{slow} and τ_{fast} of rotational relaxation. So we can say that, although the observed slow rotational relaxation (τ_{slow}) is a convolution of the relaxation time corresponding to the overall rotational motion of the micelles (τ_M) and lateral diffusion of the probe (τ_D), the contribution of overall rotational motion of the micelles (τ_M) is relatively less. To obtain the lateral diffusion coefficient, D_L we have used following equation

$$D_L = \frac{{r_h}^2}{6\tau_D} \quad (5)$$

The lateral diffusion coefficient, D_L, of C-153 in aqueous solution of 28 mM SB-16 was found to be 11.22×10^{-6} cm^2 s^{-1}. From Table 2, it is clear that with the addition of 20 mM ILs the D_L values decrease. This can be accounted for by the increase in compactness of the micelles which results from the increase in aggregation number and decrease in size of the micellar aggregates.[77] On the other hand, with further addition of ILs (800 mM) the D_L values increase which is an outcome of increased water penetration (increase in microfluidity) at higher concentration of ILs.[77]

We have also calculated the order parameter (S) from the following equation

$$S^2 = a_{slow} \quad (6)$$

where S^2 is square of the order parameter (which is a measure of the equilibrium orientational distribution of the dye).[82] The magnitude of S is a measure of spatial restriction. The magnitude of S varies from 0 (unrestricted motion) to 1 (completely restricted motion). In our case the value of S lies between 0.65 and 0.72, which is a clear indication of incorporation of C-153 molecule inside the micellar aggregate. We have also calculated the cone angle (θ_0) and wobbling diffusion coefficient (D_w) following eqs 7 and 8.

$$\theta_0 = \cos^{-1}\left[\frac{1}{2}((1 + 8S)^{1/2} - 1)\right] \quad (7)$$

$$D_W = \frac{7\theta^2}{24\tau_e} \quad (8)$$

where θ is the cone angle in radians. The values of all the above analytical parameters are tabulated in Table 2. The wobbling diffusion coefficient (D_w) of C-153 in aqueous solution of 28 mM SB-16 was found to be 3.158×10^8 s^{-1}, which increases with increasing amount of added ILs. With the addition of 800 mM $[C_2mim][C_6SO_4]$ to 28 mM aqueous SB-16 the D_w increases to 5.272×10^8 s^{-1}, which can once again be attributed to the increase in water penetration (increased microfluidity) at higher concentration of ILs.[77]

The average rotational relaxation time of C-153 at 298 K in aqueous solution of 28 mM SB-16 was found to be 1.12 ns with components 1.95 ns (48%) and 0.35 ns (52%). Interestingly, with the addition of RTILs certain counterintuitive results are obtained. It has been observed that in the presence of added RTILs the viscosity increases (Table 1), whereas the rotational relaxation becomes faster. The change in rotational relaxation is more pronounced in the case of $[C_2mim][C_6SO_4]$ addition compared to that for $[C_2mim][C_4SO_4]$ and $[C_2mim][C_2SO_4]$ addition. With the addition of 800 mM $[C_2mim][C_2SO_4]$, $[C_2mim][C_4SO_4]$, and $[C_2mim][C_6SO_4]$ to 28 mM aqueous SB-16, the average rotational relaxation time changes from 1.12 ns to 1.12, 0.70, and 0.40 ns, respectively, whereas the viscosity changes from 0.92 cP to 1.36, 1.65, and 2.18 cP, respectively. So we can clearly say that in this case the change in the rotational dynamics is not consistent with the bulk viscosity. In our earlier report,[77] we have shown that with the addition of 800 mM$[C_2mim][C_6SO_4]$ to 28 mM aqueous SB-16 the microfluidity increases drastically, whereas it remains the same in the case of $[C_2mim][C_2SO_4]$. This fact can be used in explaining the observed difference in the effects of addition of the three ionic liquids. We have determined the microviscosity (η_{mic}) inside the micellar pseudophase following the well-known Stokes−Einstein−Debye relation (eq 9)

$$\langle\tau_{rot}\rangle = \frac{\eta_{mic} V}{k_B T} \quad (9)$$

where V is the volume of the fluorophore, k_B is the Boltzmann constant, $\langle\tau_{rot}\rangle$ is the average rotational relaxation time, and T is the absolute temperature. We have determined the volume of C-153 following the method of Choudhury et al.[83] From Table 2 it is clear that the microviscosity obtained inside 28 mM aqueous solutions of SB-16 is quite large (18.8 cP) compared to bulk viscosity (0.92 cP). On the other hand, microviscosities obtained inside 28 mM aqueous solutions of SB-16 containing 800 mM $[C_2mim][C_6SO_4]$ and $[C_2mim][C_2SO_4]$ are 6.71 and 18.80 cP, respectively.

Interestingly, Kumbhakar et al.[52] have shown that ions of the added salts reside in the palisade layer, and due to the hydration of the ions, especially the cations, the water molecules in the palisade layer undergo a kind of clustering, causing the microviscosity to in fact increase rather than decrease as

dx.doi.org/10.1021/jp300544j | J. Phys. Chem. B 2012, 116, 3690−3698

expected due to increased micellar hydration. On the other hand, we can say that in our case the anion is preferentially incorporated into the micellar system and the cation is also not that efficient in bringing about water clustering, so increased micellar hydration causes decrease in microviscosity.

3.2.2. Solvation Dynamics. To study solvent relaxation dynamics, we collected the time-resolved decays monitored at different wavelengths for all the systems. In all the systems the fluorescence decays of C-153 showed huge dependence on the emission wavelength. At the red edge of emission spectra, the observed decay consists of a clear rise (growth) followed by usual decay, and at the blue end of emission spectra, a faster decay is observed which is a clear signature of the solvation dynamics. The representative decays of C-153 in 28 mM aqueous SB-16 solution, monitored at three different wavelengths at 298 K, are shown in Figure 4. The red edge and

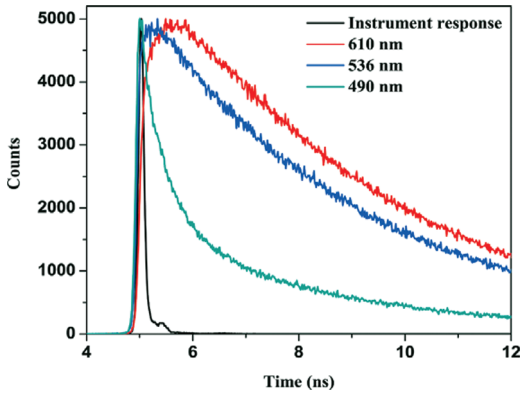

Figure 4. Fluorescence decay of C-153 in 28 mM aqueous SB-16 at three different wavelengths.

extreme blue edge decay profiles were best fitted by biexponential and triexponential functions, respectively. The time-resolved emission spectra (TRES) were constructed by the following procedure of Fleming and Maroncelli.[84,85] The TRES at a given time t, $S(\lambda;t)$, is obtained by the fitted decays, $D(t;\lambda)$, by relative normalization to the steady-state spectrum $S_0(\lambda)$, as follows

$$S(\lambda;\, t) = D(t;\, \lambda)\frac{S_0(\lambda)}{\int_0^\infty D(t;\, \lambda)\, \mathrm{d}t} \tag{10}$$

Each time-resolved emission spectrum (TRES) was fitted by "log-normal line shape function", which is defined as

$$g(\nu) = g_0 \exp\left[-\ln 2\left(\frac{\ln[1 + 2b(\nu - \nu_p)/\Delta]}{b}\right)^2\right] \tag{11}$$

where g_0, b, ν_p, and Δ are the peak height, asymmetric parameter, peak frequency, and width parameter, respectively. The representative TRES plot of C-153 in 28 mM aqueous SB-16 solution is shown in Figure 5. The peak frequency evaluated from this log-normal fitting of TRES was then used to construct the decay of the solvent correlation function $C(t)$, which is defined as

$$C(t) = \frac{\nu(t) - \nu(\infty)}{\nu(0) - \nu(\infty)} \tag{12}$$

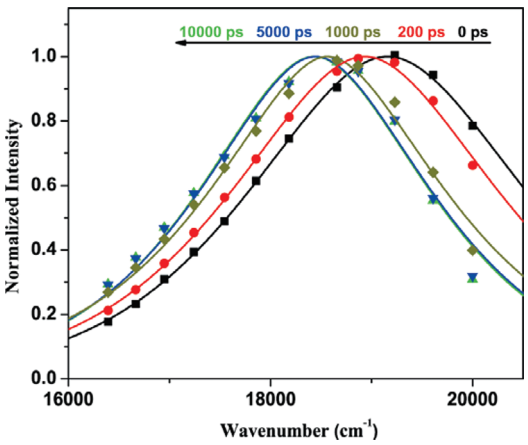

Figure 5. Time-resolved emission spectra of C-153 in 28 mM aqueous SB-16.

$\nu(0)$ is the frequency at "zero time", as calculated by the full method of Fleming and Maroncelli.[85] $\nu(\infty)$ is the frequency at "infinite time", which may be taken as the maximum of the steady-state fluorescence spectrum if solvation is more rapid than the population decay of the probe. $\nu(t)$ is determined by taking the maxima from the log-normal fits as the emission maximum. In most of the cases, however, the spectra are broad, so there is some uncertainty in the exact position of the emission maxima. Therefore, following Petrich et al.[86−88] we have considered the range of the raw data points in the neighborhood of the maximum to estimate an error for the maximum obtained from the log-normal fit. Depending on the width of the spectrum (i.e., zero time, steady state, or TRES), we have determined the typical uncertainties as follows: zero time ≈ steady state (110 cm^{-1}) < time resolved (200 cm^{-1}) emission. We use these uncertainties to compute error bars for $C(t)$. Finally, in generating $C(t)$, the first point was obtained from the zero time spectrum. The second point was taken at the maximum of the instrument response function, which, having a full width at half-maximum of ≤100 ps, was taken to be 100 ps. Finally, the time dependence of the calculated $C(t)$ values were fitted by a biexponential function because χ^2 (autocorrelation function) lies close to 1, which indicates the goodness of the fit. The biexponential function is as follows

$$C(t) = a_1 e^{-t/\tau_1} + a_2 e^{-t/\tau_2} \tag{13}$$

where τ_1 and τ_2 are the two solvation times with amplitudes of a_1 and a_2, respectively. The $C(t)$ versus time plots are shown in Figure 6. The decay parameters of $C(t)$ are summarized in Table 3. The average solvation time is calculated as

$$\tau_{av} = a_1\tau_1 + a_2\tau_2 \tag{14}$$

For explaining the solvent relaxation process in the micelle, one should take care of the fact that on going from bulk solvent to the micellar solution there is a sharp change in the dielectric constant within the molecular dimensions.[85] Accordingly, the molecular approach for the solvent relaxation process, which takes account of the solvent structures around the probe,[85,89] should be applied for understanding the results in micellar solutions. The solvation process is expected to be substantially slower in micellar media than in bulk water due to the hindered motion of water molecule inside the micelle.[4−6,20] Moreover, it is likely that the response from the few water molecules that are adjacent to the probe will be much slower than the collective

dx.doi.org/10.1021/jp300544j | J. Phys. Chem. B 2012, 116, 3690−3698

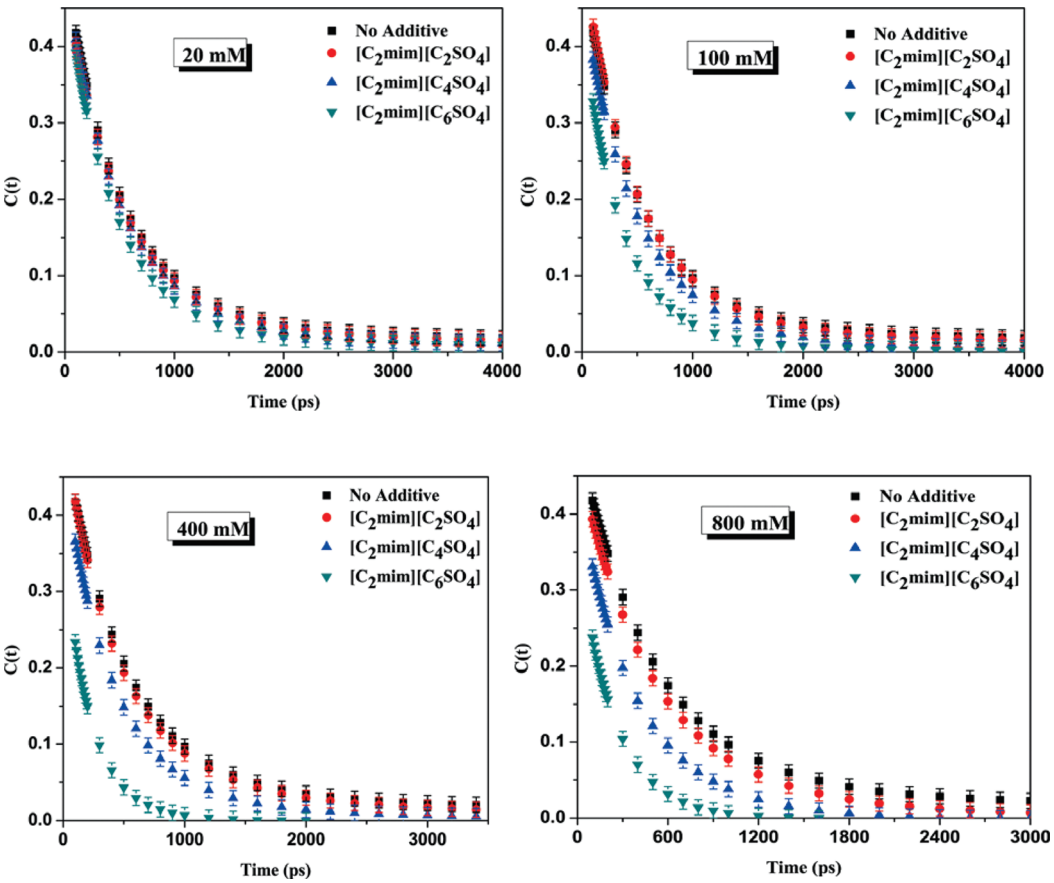

Figure 6. Decay of solvent correlation function $C(t)$ of C-153 in 28 mM aqueous SB-16 in the presence of different amounts of ILs.

Table 3. Decay Parameters of $C(t)$ of C-153 in 28 mM Aqueous SB-16 (Excluding the Missing Component) in the Presence of Different Amounts of ILs[a]

additive concn (mM)	additive	$\tau_i(a_i)$ (ns)	$\langle\tau_s\rangle^b$ (ns)
0	no additive	0.51 (0.46), 5.79 (0.04)	0.47
20	$[C_2mim][C_2SO_4]$	0.51 (0.45), 5.19 (0.04)	0.44
	$[C_2mim][C_4SO_4]$	0.48 (0.46), 3.39 (0.04)	0.36
	$[C_2mim][C_6SO_4]$	0.45 (0.46), 4.42 (0.02)	0.30
100	$[C_2mim][C_2SO_4]$	0.50 (0.48), 4.73 (0.04)	0.43
	$[C_2mim][C_4SO_4]$	0.48 (0.43), 2.12 (0.03)	0.27
	$[C_2mim][C_6SO_4]$	0.34 (0.39), 1.27 (0.04)	0.18
400	$[C_2mim][C_2SO_4]$	0.44 (0.45), 2.24 (0.06)	0.33
	$[C_2mim][C_4SO_4]$	0.39 (0.42), 1.69 (0.04)	0.23
	$[C_2mim][C_6SO_4]$	0.15 (0.14), 0.28 (0.23)	0.09
800	$[C_2mim][C_2SO_4]$	0.47 (0.43), 1.58 (0.05)	0.28
	$[C_2mim][C_4SO_4]$	0.19 (0.08), 0.45 (0.35)	0.17
	$[C_2mim][C_6SO_4]$	0.07 (0.03), 0.25 (0.34)	0.09

[a] $\langle\tau_s\rangle = a_1\tau_1 + a_2\tau_2$. [b] Error in experimental data of ±0.09 ns.

response of the water molecules that are somewhat away from the probe.[85,89] Thus, in micellar media the slower solvation component is determined mainly by the response of the few water molecules that are close to the probe and the faster solvation component is determined mainly by the collective response of a relatively large number of water molecules that are somewhat away from the probe.[21]

To get the real meaning of the solvation dynamics results, a thorough understanding of the micellar structure and location of the probe within the micelle is necessary. UV, fluorescence, and anisotropy studies showed that the probe molecules reside in the palisade layer of the micelle. The average solvation time of C-153 at 298 K in aqueous solution of 28 mM SB-16 was found to be 0.47 ns (Table 3) with components 0.51 ns (46%) and 5.79 ns (4%). It has been observed that in the presence of added RTILs the solvation dynamics becomes faster and the change in solvation dynamics is more pronounced in the case of $[C_2mim][C_6SO_4]$ compared to that for $[C_2mim][C_4SO_4]$ and $[C_2mim][C_2SO_4]$. With the addition of 800 mM $[C_2mim][C_2SO_4]$, $[C_2mim][C_4SO_4]$, and $[C_2mim][C_6SO_4]$ in 28 mM aqueous SB-16 the average solvation time changes from 0.47 ns to 0.28, 0.17, and 0.09 ns, respectively. The slow component of solvation time of C-153 at 298 K in aqueous solution of 28 mM SB-16 was found to be 5.79 ns (Table 3) with amplitude of 4%. With the addition of 800 mM $[C_2mim][C_2SO_4]$, the slow component of solvation dynamics changes from 5.79 to 1.58 ns and the amplitude changes from 4% to 5%, which clearly indicates that the strength of the hydrogen bonding decreases, whereas the penetration of water molecule almost remains same. This is in agreement with our earlier report, where we have shown that with the addition of 800 mM $[C_2mim][C_2SO_4]$ the microfluidity remains the same. With the addition of 800 mM $[C_2mim][C_6SO_4]$, the slow component of solvation dynamics changes from 5.79 to 0.25 ns and the amplitude changes from 4% to 34%, which clearly indicates that the strength of the hydrogen bonding decreases abnormally, while the penetration of water molecule increases to a great extent. This is also in agreement with our earlier report, where we have shown that with the addition of 800 mM $[C_2mim][C_6SO_4]$ the microfluidity increases drastically.[77]

dx.doi.org/10.1021/jp300544j | J. Phys. Chem. B 2012, 116, 3690−3698

If we consider the fast component of the solvation dynamics, then we can say that with the addition of 800 mM $[C_2mim][C_2SO_4]$ the fast component of solvation dynamics changes from 0.51 to 0.47 ns and the amplitude changes from 46% to 43%, which clearly indicates that the location of the probe molecule remains same. With the addition of 800 mM $[C_2mim][C_6SO_4]$, the fast component of solvation dynamics changes from 0.51 to 0.07 ns and the amplitude changes from 46% to 3%, which clearly indicates that the location of the probe m olecule changes a lot. Since with the addition of 800 mM $[C_2mim][C_6SO_4]$ the penetration of water molecule increases to a great extent, the probe in the palisade layer undergoes a relative migration toward the micellar surface, causing it to experience more polar microenvironment. Thus, the fast component of solvation is mainly due to the bulk water, which is quite fast and cannot be detected by our instrumental resolution and due to this reason the observed amplitude changes from 46% to 3%.

So these differences in the behavior of three ionic liquids can be accounted for by our earlier report,[77] where we have proposed that in the case of $[C_2mim][C_6SO_4]$ the presence of hexyl chain on the hexyl sulfate ion allows it to align with the tail part of the SB-16, whereas in the case of $[C_2mim][C_2SO_4]$ the presence of ethyl chain in the ethyl sulfate ion is apparently unable to align the ethyl sulfate anion with the tail part of the SB-16. In our earlier publication, the change in ζ potential with the addition of ILs has been recorded to prove our proposition. The ζ potential of the SB-16 micelle in sodium tetraborate buffer (pH = 9.0) was found to be −24.0 mV which decreased to −69.0 and −31.2 mV with addition of 20 mM $[C_2mim][C_6SO_4]$ and $[C_2mim][C_2SO_4]$, respectively.[77] As stated in the aforementioned report, this rapid increase of negative ζ potential with the addition of $[C_2mim][C_6SO_4]$ indicates very strong interactions of $[C_2mim][C_6SO_4]$ with quaternary ammonium ions of SB-16 micellar aggregates which lead to more anionoid SB-16 micellar aggregates.[77] This difference in the location of the anions of ILs and hence the difference in the water penetration level is responsible for the different behaviors of the ILs. Kumbhakar et al.[52] have shown that ions of the added salts reside in the palisade layer, and due to the hydration of the ions, especially the cations, the water molecules in the palisade layer undergo a kind of clustering, and thereby the mobility of these molecules decreases. In contrast, our results reflect that the anion is preferentially incorporated into the micellar system and since the cation is not that effective in producing water clustering, there is increased micellar hydration which causes increase in mobility.

4. CONCLUSION

In conclusion, we can say that the solvent and rotational relaxation of C-153 at 298 K in aqueous solution of 28 mM SB-16 become faster with the addition of the RTILs $[C_2mim][C_2SO_4]$, $[C_2mim][C_4SO_4]$, and $[C_2mim][C_6SO_4]$. Among these three ILs, the most pronounced change in solvent and rotational relaxation of C-153 is observed in the case of $[C_2mim][C_6SO_4]$. As stated in our earlier report,[77] the hexyl chain on the hexyl sulfate ion is responsible for the more pronounced penetration of the hexyl sulfate anion of $[C_2mim][C_6SO_4]$ because it aids in aligning the anion with the tail part of SB-16. But in the case of $[C_2mim][C_2SO_4]$, the ethyl chain in the ethyl sulfate ion is apparently unsuccessful in functioning similarly and the ethyl sulfate anion is unable to align itself with the tail part of SB-16. It is this difference in the location of the anions of ILs and the resulting difference in the water penetration level that is responsible for the different behavior of ILs. So we can say that our investigation has outlined the unique role of different ILs and their concentration dependence in modifying the properties of water molecules in the palisade layer of an aqueous zwitterionic micellar solution. We have certainly established a class of hybrid environmentally benign systems made up of IL-modified aqueous surfactants. This type of zwitterionic micelles where the ionic liquids get incorporated inside the micelle may have enormous future application for conducting interfacial reactions and micellar catalysis.

AUTHOR INFORMATION

Corresponding Author

*E-mail: nilmoni@chem.iitkgp.ernet.in. Fax: 91-3222-255303.

Notes

The authors declare no competing financial interest.

ACKNOWLEDGMENTS

N.S. thanks the Council of Scientific and Industrial Research (CSIR), and the Board of Research in Nuclear Sciences (BRNS), Government of India, for generous research grants. V.G.R., C.G., S.G., and S.M. thank CSIR for a research fellowship. We thank Ms. Udita Brahmachari for the English correction of the manuscript.

REFERENCES

(1) Pratt, L. R.; Pohorille, A. *Chem. Rev.* **2002**, *102*, 2671−2691.
(2) See papers on Hydration Processes in Biological and Macromolecular Systems. *Faraday Discuss.* **1996**, *103*, 1−18.
(3) Benjamin, I. *Chem. Rev.* **1996**, *96*, 1449−1475.
(4) Nandi, N.; Bhattacharyya, K.; Bagchi, B. *Chem. Rev.* **2000**, *100*, 2013−2046.
(5) Bagchi, B. *Chem. Rev.* **2005**, *105*, 3197−3219.
(6) Bagchi, B.; Jana, B. *Chem. Soc. Rev.* **2010**, *39*, 1936−1954.
(7) Halle, B. *Philos. Trans. R. Soc., London B* **2004**, *359*, 1207−1224.
(8) Kumbhakar, M.; Nath, S.; Pal, H.; Sapre, A. V.; Mukherjee, T. *J. Chem. Phys.* **2003**, *119*, 388−399.
(9) Kumbhakar, M.; Nath, S.; Mukherjee, T.; Pal, H. *J. Chem. Phys.* **2004**, *120*, 2824−2834.
(10) Fukuzumi, S.; Nishimine, M.; Ohkubo, K.; Tkachenko, N. V.; Lemmetyinen, H. *J. Phys. Chem. B* **2003**, *107*, 12511−12518.
(11) Fendler, J. H. *Membrane Mimetic Chemistry*; Wiley: New York, 1982.
(12) Gratzel, M. *Heterogeneous photochemical electron transfer*; CRC Press: Boca Raton, FL, 1989.
(13) Sarkar, N.; Datta, A.; Das, S.; Bhattacharyya, K. *J. Phys. Chem.* **1996**, *100*, 15483−15486.
(14) Hara, K.; Kuwabara, H.; Kajimoto, O. *J. Phys. Chem. A* **2001**, *105*, 7174−7179.
(15) Kumbhakar, M.; Nath, S.; Mukherjee, T.; Pal, H. *J. Chem. Phys.* **2004**, *121*, 6026−6033.
(16) Sen, P.; Mukherjee, S.; Halder, A.; Bhattacharyya, K. *Chem. Phys. Lett.* **2004**, *385*, 357−361.
(17) Willard, D. M.; Riter, R. E.; Levinger, N. E. *J. Am. Chem. Soc.* **1998**, *120*, 4151−4160.
(18) Riter, R. E.; Undiks, E. P.; Levinger, N. E. *J. Am. Chem. Soc.* **1998**, *120*, 6062−6067.
(19) Sarkar, N.; Dutta, A.; Das, S.; Bhattacharyya, K. *J. Phys. Chem.* **1996**, *100*, 10523−10527.
(20) Bhattacharyya, K.; Bagchi, B. *J. Phys. Chem. A* **2000**, *104*, 10603−10613.
(21) Nandi, N.; Bagchi, B. *J. Phys. Chem. B* **1997**, *101*, 10954−10961.
(22) Bhattacharyya, K. *Acc. Chem. Res.* **2003**, *36*, 95−101.

(23) Pal, S. K.; Peon, J.; Bagchi, B.; Zewail, A. H. *J. Phys. Chem. B* **2002**, *106*, 12376−12395.
(24) Bagchi, B. *Annu. Rep. Prog. Chem., Sect. C* **2003**, *99*, 127−175.
(25) Jimenez, R.; Fleming, G. R.; Kumar, P. V.; Maroncelli, M. *Nature* **1994**, *369*, 471−473.
(26) Sen, S.; Dutta, P.; Sukul, D.; Bhattacharyya, K. *J. Phys. Chem. A* **2002**, *106*, 6017−6023.
(27) Sahu, K.; Roy, D.; Mondal, S. K.; Halder, A.; Bhattacharyya, K. *J. Phys. Chem. B* **2004**, *108*, 11971−11975.
(28) Riter, R. E.; Willard, D. M.; Levinger, N. E. *J. Phys. Chem. B* **1998**, *102*, 2705−2714.
(29) Hara, K.; Baden, N.; Kajimoto, N. *J. Phys.: Condens. Matter* **2004**, *16*, S1207.
(30) Chakrabarty, D.; Hazra, P.; Chakraborty, A.; Sarkar, N. *J. Phys. Chem. B* **2003**, *107*, 13643−13648.
(31) Pal, S. K.; Peon, J.; Zewail, A. H. *Proc. Natl. Acad. Sci. U.S.A.* **2002**, *99*, 1763−1768.
(32) Bruce, C. D.; Senapati, S.; Berkowitz, M. L.; Perera, L.; Forbes, M. D. E. *J. Phys. Chem. B* **2002**, *106*, 10902−10907.
(33) Balasubramanian, S.; Bagchi, B. *J. Phys. Chem. B* **2002**, *106*, 3668−3672.
(34) Balasubramanian, S.; Bagchi, B. *J. Phys. Chem. B* **2001**, *105*, 12529−12533.
(35) Faeder, J.; Ladanyi, B. M. *J. Phys. Chem. B* **2000**, *104*, 1033−1046.
(36) Faeder, J.; Ladanyi, B. M. *J. Phys. Chem. B* **2001**, *105*, 11148−11158.
(37) Dastidar, S. G.; Mukhopadhyay, C. *Phys. Rev. E* **2003**, *68*, 021921−021929.
(38) Dastidar, S. G.; Mukhopadhyay, C *Phys. Rev. E* **2004**, *70*, 061901−061909.
(39) Pal, S.; Bagchi, B.; Balasubramanian, S. *J. Phys. Chem. B* **2005**, *109*, 12879−12890.
(40) Tarek, M.; Tobias, D. J. *Phys. Rev. Lett.* **2002**, *88*, 138101−138104.
(41) Smith, J. C.; Merzel, F.; Verma, C. S.; Fischer, S. *J. Mol. Liq.* **2002**, *101*, 27−33.
(42) Melchionna, S.; Briganti, G.; Londei, P.; Cammarano, P. *Phys. Rev. Lett.* **2004**, *92*, 158101−158104.
(43) Russo, D.; Hura, G.; Head-Gordon, T. *Biophys. J.* **2004**, *86*, 1852−1862.
(44) Bandyopadhyay, S.; Chakraborty, S.; Balasubramanian, S.; Pal, S.; Bagchi, B. *J. Phys. Chem. B* **2004**, *108*, 12608−12616.
(45) Pal, S.; Balasubramanian, S.; Bagchi, B. *J. Phys. Chem. B* **2003**, *107*, 5194−5202.
(46) Bandyopadhyay, S.; Tarek, M.; Klein, M. L. *Curr. Opin. Colloid Interface Sci.* **1998**, *3*, 242−246.
(47) Tarek, M.; Bandyopadhyay, S.; Klein, M. L. *J. Mol. Liq.* **1998**, *78*, 1.
(48) Altschuler, M.; Heddens, D. K.; Diveley, R. R.; Krescheck, G. C. *BioTechniques* **1994**, *17*, 434−436.
(49) Kresheck, G. C.; Hwang, J. *J. Chem. Phys. Lipids* **1995**, *76*, 193−199.
(50) Patra, K. S.; Alonso, A.; Goni, F. M. *Biochim. Biophys. Acta* **1998**, *1373*, 112−118.
(51) Robson, R. J.; Dennis, E. A. *Biochim. Biophys. Acta* **1978**, *508*, 513−524.
(52) Kumbhakar, M.; Goel, T.; Mukherjee, T.; Pal, H. *J. Phys. Chem. B* **2005**, *109*, 14168−14174.
(53) Christov, N. C.; Denkov, N. D.; Kralchevsky, P. A.; Ananthapadmanabhan, K. P.; Lips, A. *Langmuir* **2004**, *20*, 565−571.
(54) Danov, K. D.; Kralchevska, S. D.; Kralchevsky, P. A.; Ananthapadmanabhan, K. P.; Lips, A. *Langmuir* **2004**, *20*, 5445−5453.
(55) Bartolo, R. G. Soap. In *Encyclopedia of Chemical Technology*, 4th ed.; Kroschwitz, J. I., Ed.; Wiley Interscience: New York, 1993; pp 297−326.
(56) Pillersdorf, A.; Katzhendler, J. *Isr. J. Chem.* **1979**, *18*, 330−338.
(57) Bunton, C. A.; Mhala, M. M.; Moffatt, J. R. *J. Phys. Chem.* **1989**, *93*, 854−858.
(58) Lee, B.; Nome, F. *Langmuir* **2000**, *16*, 10131−10136.
(59) Chevalier, J.; Kamenka, N.; Chorro, M.; Zana, R. *Langmuir* **1996**, *12*, 3225−3232.
(60) Weers, J.; Rathman., J.; Axe, F.; Crichlow, C.; Foland, L.; Scheuing, D.; Wiersema, R.; Zielske, A. *Langmuir* **1991**, *7*, 854−867.
(61) Savelli, G.; Germani, R.; Brinchi, L. In *Reactions and Synthesis in Surfactants Systems*; Texter, J., Ed.; Marcel Dekker: New York, 2001; Chapter 8.
(62) Iso, K.; Okada, T. *Langmuir* **2000**, *16*, 9199−9204.
(63) Marte, L.; Beber, R. C.; Farrukh, M. A.; Micke, G. A.; Costa, A. C. O.; Gillitt, N. D.; Bunton, C. A; Profio, P. D.; Savelli, G.; Nome, F. *J. Phys. Chem. B* **2007**, *111*, 9762−9769.
(64) Tondo, D. W.; Priebe, J. M.; Souza, B. S.; Priebe, J. P.; Bunton, C. A.; Nome, F. *J. Phys. Chem. B* **2007**, *111*, 11867−11869.
(65) Kamenka, K.; Chorro, M.; Chevalier, Y.; Levy, H.; Zana, R. *Langmuir* **1995**, *11*, 4234−4240.
(66) Cuccovia, I. M.; Romsted, L. S.; Chaimovich, H. *J. Colloid Interface Sci.* **1999**, *220*, 96−102.
(67) Profio, D. P.; Germani, R.; Savelli, G.; Cerichelli, G.; Chiarini, M.; Mancini, G.; Bunton, C. A.; Gillit, N. D. *Langmuir* **1998**, *14*, 2662−2669.
(68) Jiang, W.; Irgum, K. *Anal. Chem.* **1999**, *71*, 333−344.
(69) Jiang, W.; Irgum, K. *Anal. Chem.* **2001**, *73*, 1993−2003.
(70) Moore, L.; LeJeune, Z. M.; Luces, C. A.; Gates, A. T.; Li, M.; El-Zahab, B.; Garno, J. C.; Warner, I. M. *Anal. Chem.* **2010**, *82*, 3997−4005.
(71) Priebe, J. P.; Souza, B. S.; Micke, G. A.; Costa, A. C. O.; Fiedler, H. D.; Bunton, C. A.; Nome, F. *Langmuir* **2010**, *26*, 1008−1012.
(72) Priebe, J. P.; Satnami, M. L.; Tondo, D. W.; Souza, B. S.; Priebe, J. M.; Micke, G. A.; Costa, A. C. O.; Fiedler, H. D.; Bunton, C. A.; Nome, F. *J. Phys. Chem. B* **2008**, *112*, 14373−14378.
(73) Behera, K.; Pandey, S. *J. Phys. Chem. B* **2007**, *111*, 13307−13315.
(74) Behera, K.; Pandey, M. D.; Porel, M.; Pandey, S. *J. Chem. Phys.* **2007**, *127*, 184501−184510.
(75) Behera, K.; Om, H.; Pandey, S. *J. Phys. Chem. B* **2009**, *113*, 786−793.
(76) Behera, K.; Pandey, S. *Langmuir* **2008**, *24*, 6462−6469.
(77) Rao, V. G.; Ghatak, C.; Ghosh, S.; Mandal, S.; Sarkar, N. *Chem. Phys. Chem.* (DOI: 10.1002/cphc.201100866).
(78) Hazra, P.; Sarkar, N. *Chem. Phys. Lett.* **2001**, *342*, 303−311.
(79) Hazra, P.; Chakrabarty, D.; Sarkar, N. *Langmuir* **2002**, *18*, 7872−7879.
(80) Hazra, P.; Chakrabarty, D.; Sarkar, N. *Chem. Phys. Lett.* **2003**, *371*, 553−562.
(81) Quitevis, E. L.; Marcus, A. H.; Fayer, M. D. *J. Phys. Chem.* **1993**, *97*, 5762−5769.
(82) Lipari, G.; Szabo, A. *Biophys. J.* **1980**, *30*, 489−506.
(83) Choudhury, S. D.; Kumbhakar, M.; Nath, S.; Pal, H. *J. Chem. Phys.* **2007**, *127*, 194901−194913.
(84) Maroncelli, M.; Fleming, G. R. *J. Chem. Phys.* **1987**, *86*, 6221−6239.
(85) Fee, R. S.; Maroncelli, M. *Chem. Phys.* **1994**, *183*, 235−247.
(86) Bose, S.; Adhikary, R.; Mukherjee, P.; Song, X.; Petrich, J. W. *J. Phys. Chem. B* **2009**, *113*, 11061−11068.
(87) Headley, L. S.; Mukherjee, P.; Anderson, J. L.; Ding, R.; Halder, M.; Armstrong, D. W.; Song, X.; Petrich, J. W. *J. Phys. Chem. A* **2006**, *110*, 9549−9554.
(88) Mukherjee, P.; Crank, J. A.; Sharma, P. S.; Wijeratne, A. B.; Adhikary, R.; Bose, S.; Armstrong, D. W.; Petrich, J. W. *J. Phys. Chem. B* **2008**, *112*, 3390−3396.
(89) Maroncelli, M.; MacInnis, J.; Fleming, G. R. *Science* **1989**, *243*, 1674−1681.